Mon. Not. R. Astron. Soc. **398,** 1582–1592 (2009) doi:10.1111/j.1365-2966.2009.15226.x

Optical spectroscopy of X-Mega targets in the Carina nebula – VII. On the multiplicity of Tr 16-112, HD 93343 and HD 93250★

G. Rauw,[1]†‡ Y. Nazé,[1]§ E. Fernández Lajús,[2] A. A. Lanotte,[1] G. R. Solivella,[2] H. Sana[3] and E. Gosset[1]¶

[1] *Institut d'Astrophysique & Géophysique, Université de Liège, Bât. B5c, Allée du 6 Août 17, B-4000 Liège, Belgium*
[2] *Facultad de Ciencias Astronómicas y Geofísicas, Universidad Nacional de La Plata, Paseo del Bosque S/N, 1900 La Plata, Argentina*
[3] *European Southern Observatory, Alonso de Cordova 3107, Vitacura, Santiago 19, Chile*

Accepted 2009 June 9. Received 2009 June 2; in original form 2009 April 23

ABSTRACT

We present the results of a spectroscopic monitoring campaign devoted to three O-type stars in the Carina nebula. We derive the full SB2 orbital solution of the binary system Tr 16-112, an exceptional dissymmetrical system consisting of an O5.5–6 V((f$^+$?p)) primary and a B2 V-III secondary. We also report on low-amplitude brightness variations in Tr 16-112 that are likely due to the ellipsoidal shape of the O5.5–6 primary revolving in an eccentric orbit around the system's centre of mass. We detect for the first time a clear SB2 binary signature in the spectrum of HD 93343 (O8 + O8), although our data are not sufficient to establish an orbital solution. This system also displays low-amplitude photometric modulations. On the other hand, no indication of multiplicity is found in the optical spectra of HD 93250. Finally, we discuss the general properties of multiple massive stars in the Carina OB1 association.

Key words: binaries: spectroscopic – stars: early-type – stars: fundamental parameters – stars: individual: Tr 16-112 – stars: individual: HD 93343 – stars: individual: HD 93250.

1 INTRODUCTION

The investigation of the multiplicity of early-type stars in very young open clusters is a powerful tool to better understand many problems related to massive star research. First of all, such studies allow us to enlarge the – still rather small – sample of massive stars with well-determined fundamental properties such as masses and radii. Moreover, the statistical properties of the binary systems also constrain the formation scenarios of massive stars (see e.g. Sana et al. 2008).

The region around η Carinae harbours several very young open clusters and is therefore extremely rich in early-type stars. As a consequence, this area has been the subject of many investigations over the last 30 yr. In this context and in the framework of the so-called X-Mega project (Corcoran et al. 1999), aiming (among other things) at an intensive monitoring of the region around η Carinae with the *ROSAT* X-ray satellite, a large multiwavelength observing effort was devoted to the Carina nebula and the Trumpler 16 cluster in particular. One of the prime objectives was to obtain accurate ephemerides of colliding-wind early-type binary systems to interpret their X-ray light curves. The spectroscopic monitoring of these objects started in the late 1990s and led to a series of papers (Albacete Colombo et al. 2001, 2002; Morrell et al. 2001; Rauw et al. 2001; Nazé et al. 2005; Niemela et al. 2006, hereafter Paper I, Paper IV, Paper II, Paper III, Paper V and Paper VI, respectively) reporting the results of dedicated investigations of the properties of a number of O-type binaries in the Carina nebula. This paper is the seventh in this series and is devoted to three objects: the binary systems Tr 16-112 and HD 93343 as well as the likely single star HD 93250. Furthermore, we briefly discuss the general properties of O-type binaries in and around Trumpler 16 as derived in the framework of the present campaign and other related studies.

2 OBSERVATIONS

2.1 Medium-resolution spectroscopy

Six medium-resolution spectra of Tr 16-112 and HD 93343 in the wavelength range 3850–4800 Å were gathered in 1997 with the European Southern Observatory (ESO) 1.5-m telescope equipped with a Boller & Chivens (B&C) Cassegrain spectrograph (see

★Based on observations collected at the European Southern Observatory (La Silla, Chile), at Complejo Astronómico El Leoncito (Argentina), at the Cerro Tololo Inter-American Observatory (CTIO) and with *XMM–Newton*, an ESA Science Mission with instruments and contributions directly funded by ESA Member States and the USA (NASA).

†E-mail: rauw@astro.ulg.ac.be
‡Research Associate FRS/FNRS (Belgium).
§Postdoctoral Researcher FRS/FNRS (Belgium).
¶Senior Research Associate FRS/FNRS (Belgium).

Paper III for a detailed description of the instrumentation and the data reduction).

Several spectra of Tr 16-112 were obtained in 1986 with the Cassegrain spectrograph at the CTIO 1-m telescope equipped with a two-dimensional, photon-counting detector (2D-frutti). The wavelength coverage was from 3800 to 5000 Å with a 3-pixel resolution of 1.5 Å. The signal-to-noise ratios (S/N) were about 50. Several low-resolution spectra of the same star were obtained in 1993, 2007 and 2008 at Complejo Astronómico El Leoncito (Casleo)[1], Argentina. The spectra were taken with the modified REOSC SEL[2] spectrograph in simple dispersion Cassegrain mode attached to the 2.15-m Jorge Sahade telescope. The dispersion was 1.64 Å per pixel. The data cover the wavelength range from 3800 to 4800 Å and have a S/N ratio of about 200. The spectra were reduced at Facultad de Ciencias Astronómicas y Geofísicas (Universidad Nacional de La Plata) with the IRAF[3] software version 2.10. Radial velocities (RVs) of the He II λ 4542 and λ 4686 lines were obtained by fitting a Gaussian profile to the observed lines.

2.2 High-resolution echelle spectroscopy

During several observing campaigns (1999 May, 2000 May, 2001 May, 2002 March and April, and 2004 May), we took a series of echelle spectra of our targets (27 for Tr 16-112, 9 for HD 93343 and 6 for HD 93250) with the Fiber-fed Extended Range Optical Spectrograph (FEROS) mounted first on the ESO 1.5-m (until 2002 October) and later on the ESO/MPG 2.2-m telescopes at La Silla. These spectra cover the wavelength domain from about 3750 to 9000 Å with a resolving power of 48 000. The detector was an EEV CCD with 2048 × 4096 pixels of size 15 × 15 μm^2. The exposure times were typically 30 min and the typical S/N ratios were about 150. The data were reduced using the specific context under the MIDAS environment along with an improved reduction pipeline (see Sana et al. 2003). Finally, the FEROS spectra were normalized to the continuum using polynomials.

High-resolution echelle spectra were also obtained at Casleo in 1994 and 2008 with the REOSC SEL instrument in echelle mode attached to the 2.15-m telescope. The detector was a Tek 1024 × 1024 pixel CCD. The spectra cover the wavelength range from 3600 to 6000 Å with a spectral resolving power of 18 000. Typical S/N ratios are about 80. The REOSC echelle spectra were reduced using IRAF routines. Individual echelle orders were normalized using carefully chosen continuum windows.

2.3 Photometry of Tr 16-112

CCD photometry of Tr 16-112 was performed during the nights of 2007 February 21–27, using the CH-250 camera with a PM512 CCD chip, attached to the 0.6-m Helen Sawyer Hogg telescope (f/15 Cassegrain) at Casleo. We used a standard Johnson–Cousins *B V R I* filter set for the observations, although the bulk of the data were taken in the *V* band. The CCD images were calibrated in the standard way using bias, dark and flat-field frames and finally the photometry was derived using the APPHOT/IRAF package. The typical uncertainty on the differential *V*-band photometry of Tr 16-112 is about 0.005 mag.

[1]Casleo is operated under agreement between CONICET and the National Universities of La Plata, Córdoba and San Juan.

[2]Spectrograph Echelle Liège (jointly built by REOSC and Liège Observatory and on long-term loan from the latter).

[3]IRAF is distributed by NOAO, operated by AURA, Inc., under agreement with NSF.

3 INTERSTELLAR LINES

We added up all the FEROS spectra of our targets in the wavelength domain 3870–3950 Å to derive high-quality spectra of the interstellar He I λ 3889 and Ca II K lines. For all three stars, the profiles of the Ca II K lines look remarkably similar to the plots given by Walborn (1982). The high signal to noise ratio of our mean spectra allows us to further detect some weak [equivalent widths (EWs) of a few mÅ] higher velocity components that were not seen in the older data. In the case of Tr 16-112, we definitely find a component at $-143\,\mathrm{km\,s^{-1}}$ and possibly another one at $+205\,\mathrm{km\,s^{-1}}$. In HD 93343, we clearly identify an absorption at $-75\,\mathrm{km\,s^{-1}}$, whilst in HD 93250 we detect a component at $-98\,\mathrm{km\,s^{-1}}$. All three stars display a moderately prominent interstellar He I λ3889 absorption line at a heliocentric velocity of $-28.0\,\mathrm{km\,s^{-1}}$ (for Tr 16-112 and HD 93250) and $-25.4\,\mathrm{km\,s^{-1}}$ (HD 93343). The EWs of these features are 0.010 (HD 93343), 0.045 (HD 93250) and 0.080 Å (Tr 16-112).

4 THE O + B BINARY TR 16-112

Tr 16-112 (≡ CPD −59° 2641 ≡ CD −59° 3310; Feinstein, Marraco & Muzzio 1973) is a member of the Tr 16 cluster. Based on 10 low-resolution spectra, Levato et al. (1991) classified Tr 16-112 as an SB1 binary system with an orbital period of 4.02 d. Their preliminary orbital solution yielded a significant eccentricity of 0.23. Luna et al. (2003) subsequently obtained five additional RV data points from echelle spectra and recomputed an SB1 orbital solution with a period of 4.080 d and $e = 0.25 \pm 0.03$.

4.1 The spectral types

We have applied a disentangling method based on the principles discussed by González & Levato (2006) to the normalized FEROS spectra of Tr 16-112. For this purpose, we have selected two wavelength domains within the spectral range covered by the FEROS data: our violet and blue domains cover, respectively, the wavelength intervals [4000, 4250] and [4410,4790]. Disentangling the spectra of the components of this star was a challenging task that pushed our code to its limits. Indeed, the secondary star contributes only about 8 per cent of the total light of the system making it rather difficult to accurately follow its spectral signature.

The resulting separated spectra are displayed in Fig. 1. Although the disentangled secondary spectrum is admittedly of poor quality, these spectra reveal some interesting features. The apparent EWs (i.e. with respect to the combined primary + secondary continuum) of the He I λ 4471 line as determined from the mean disentangled spectra are 0.325 ± 0.005 and 0.073 Å for the primary and secondary, respectively. For the He II λ 4542 and λ 4686 lines, the apparent primary's EWs are 0.668 ± 0.005 and 0.426 Å, respectively. None of the latter lines is seen in the secondary spectrum (see Fig. 1).

The He I λ 4471/He II λ 4542 EW ratio ($\log W' = -0.313 \pm 0.007$; see Conti 1973b and Mathys 1988) places the primary star at the border between spectral types O5.5 and O6. The disentangled primary spectrum reveals a weak, but definite, emission blend of N III λλ 4634-41 as well as a comparably strong C III λλ 4647-50

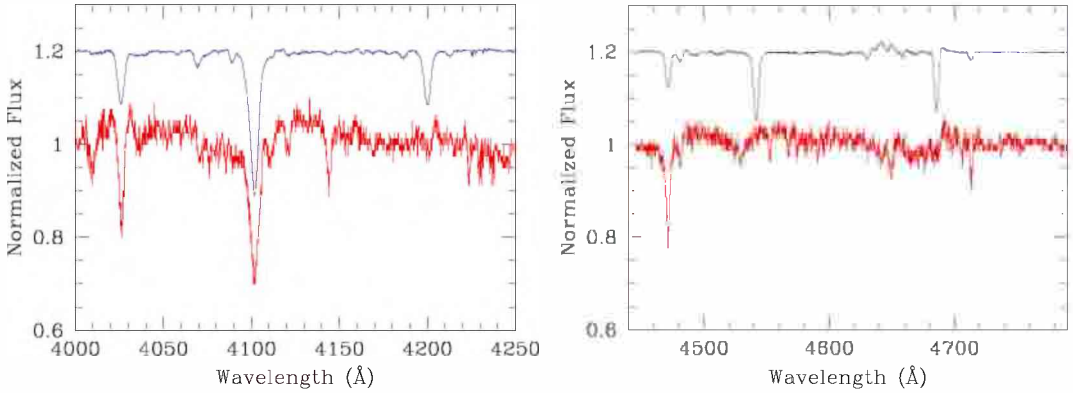

Figure 1. The normalized disentangled violet (left) and blue (right) spectra of the primary and secondary components of Tr 16-112. The disentangled spectra were normalized accounting for a brightness ratio (secondary/primary) of 0.09. For clarity, the primary spectrum was shifted upwards by 0.2 continuum units.

emission and a weak C IV λ 4658 P-Cygni profile[4]. The fact that the strength of the C III λλ 4647-50 and N III λλ 4634-41 blends are very much comparable would put the primary into the scarce category of Of?p stars (see Walborn 1972, 1973 and Nazé, Walborn & Martins 2008). We caution, however, that the known members of the Of?p category exhibit supergiant-like features and often display strong spectroscopic variability (see Nazé et al. 2008). In our data, we find no evidence for such features in the spectrum of the primary star of Tr 16-112. The He II λ 4686 absorption displays a slightly asymmetric profile with some hints of a weak P-Cygni type emission component. Some evidence for weak S IV λλ 4486, 4504 emissions as well as a very weak Si IV λ 4116 emission is found, whilst Si IV λ 4089 is clearly seen in absorption. These features motivate a spectral classification of the primary as O5.5-6 V((f$^+$?p)).

Using the Fourier transform method (see Simón-Díaz & Herrero 2007), we have determined the projected rotational velocity $v \sin i = (170 \pm 5)$ km s^{-1} from the He II λλ 4200, 4542 and O III λ 5592 lines in the disentangled primary spectrum. This value is slightly lower than the values previously determined from the composite *International Ultraviolet Explorer* (*IUE*) spectra of the system (195 and 184 km s^{-1}; see Penny 1996 and Howarth et al. 1997, respectively). One reason for this difference could be blending effects with the secondary's spectrum in the *IUE* data, as Penny mentioned the possible presence of the secondary signature in the cross-correlation function.

The lack of He II lines in the spectrum of the secondary indicates that this is a B-type star. The most prominent features in the disentangled secondary spectrum are the He I lines (λλ 4009, 4026, 4121, 4144, 4471, 4713) as well as Hδ. Somewhat weaker features are due to the C III + O II blends at 4070 and 4650 Å, as well as the Si III λλ 4552, 4568, Mg II λ 4481, N II λ 4530 and O II λ 4110 lines. The presence of a very weak Si IV λ 4089 absorption cannot be ruled out. The relative strength of the lines of the silicon ions and the strength of the Mg II line compared to He I λ 4471 suggest a spectral type B2 (or slightly earlier) with an uncertainty of about half a subclass (see Walborn & Fitzpatrick 1990). The relative strength of the N II λ 4530 line argues for a V-III luminosity class (see the luminosity effects at spectral type B2 in Walborn & Fitzpatrick 1990).

To evaluate the brightness ratio between the components of the system, we have compared the EWs of prominent lines as measured in the combined spectrum to the typical EWs of presumably single stars of the same spectral type. For the primary, we used the He I λλ 4026, 4471 as well as He II λλ 4200, 4542 lines and we took the typical values of the EWs from the paper of Conti (1973a). For the secondary, our comparison was based on the He I λλ 4026, 4471 and Mg II λ 4481 lines and the typical values of the EWs of B2 V stars given by Didelon (1982). This comparison shows that the secondary contributes about 8 ± 3 per cent of the total light of Tr 16-112 in the blue–violet spectral domain (i.e. the brightness ratio secondary/primary amounts to 0.09).

The disentangling code offers the possibility of simultaneously determining the RVs of the binary components (see Table 1). For this purpose, we used the lines listed in Table 2.

4.2 The orbital solution

Since the spectral signature of the secondary component of Tr 16-112 is rather weak, we started by treating the system as an SB1 binary. We thus measured the RVs of the primary component by fitting Gaussian line profiles to the strongest lines. It was only on a few FEROS spectra that we directly noted the presence of the secondary's spectral signature in the He I lines. In the latter cases, we simultaneously fitted two Gaussian profiles. Since the secondary is of a significantly later spectral type than the primary, the He II lines were not affected and we thus consider that the RVs of the He II lines best reflect the motion of the primary of Tr 16-112. In this way, we obtained a time series of 48 RV measurements from high-resolution echelle spectra, spanning almost 9 yr (3259 d). Note that the RV dispersion of the diffuse interstellar band (DIB) at 5780 Å in the FEROS spectra of Tr 16-112, was found to be 2.3 km s^{-1}. This value can be seen as an estimate of the uncertainty on the RV of a constant spectral line in the spectrum of this star.

We then used the generalized periodogram Fourier technique discussed by Heck, Manfroid & Mersch (1985) and Gosset et al. (2001) as well as the trial period method of Lafler & Kinman (1965) to perform a period search on the primary RVs. Previous attempts to determine the orbital period from a subset of the data discussed here revealed a severe ambiguity between a period of almost exactly 4.0 d and its alias at 1.3 d. To get rid of the aliasing problem, we thus obtained several spectra during the same night in the course of the 2001 May FEROS campaign and during the Casleo campaigns in 2008. The periodogram built from the new FEROS + Casleo data now clearly reveals its highest peak at a frequency of (0.24902 ± 0.00003) d^{-1} corresponding to an orbital period of (4.0157 ± 0.0005) d. Our value is in excellent agreement with the

[4]From its wavelength, we can actually rule out that the absorption component of this P-Cygni profile would be due to a blend with the Si IV λ 4654 absorption.

Table 1. RVs of Tr 16-112 as measured on our high-resolution echelle spectra. The first column yields the date of the observation. The second column indicates the primary RV as inferred from the direct measurement of the He II lines. Columns 3 and 4 yield the primary and secondary RVs as inferred from the disentangling method. Finally, the last column indicates the instrument that was used for the observation: FEROS (F) or the Casleo (C) SEL echelle spectrograph.

HJD−245 0000	RV_p (He II) (km s^{-1})	RV_p (km s^{-1})	RV_s (km s^{-1})	Inst.
1299.624	95.9	90.3	−374.8	F
1300.630	7.1	2.2	−7.7	F
1301.562	−79.2	−82.3	214.9	F
1301.724	−77.2			F
1302.583	−44.5	−49.9	123.4	F
1304.606	3.1	1.5	−17.3	F
1327.643	103.5	101.8	−317.9	F
1669.632	62.9	65.9	−217.0	F
1670.579	−57.5			F
1672.568	45.5	46.2	−171.9	F
2037.575	−22.2	−27.9	101.1	F
2037.690	−2.7			F
2038.531	107.1	101.7	−370.5	F
2039.594	−5.3			F
2040.603	−72.7	−79.7	287.4	F
2040.655	−74.7	−78.9	268.3	F
2335.682	105.4	96.9	−382.6	F
2337.661	−78.4	−82.3	260.2	F
2338.672	−33.1	−39.7	105.8	F
2339.674	102.2	96.5	−384.8	F
2382.533	−58.9	−63.4	208.3	F
2383.536	73.7	72.1	−257.6	F
3130.530	77.7	72.5	−284.1	F
3131.531	37.8	40.0	−156.1	F
3132.524	−69.0	−70.7	234.9	F
3133.512	−60.5			F
3134.540	78.6	75.0	−276.7	F
3135.514	38.9	36.1	−177.3	F
4474.780	−59.4			C
4474.802	−61.6			C
4475.704	67.6			C
4475.726	63.8			C
4476.723	74.8			C
4476.745	55.0			C
4477.725	−62.5			C
4477.747	−92.2			C
4524.780	66.3			C
4524.803	64.7			C
4526.513	−66.9			C
4526.539	−78.7			C
4555.567	−4.3			C
4555.589	7.4			C
4556.556	113.8			C
4556.578	104.0			C
4557.598	−36.7			C
4557.620	−33.8			C
4558.626	−80.5			C
4558.648	−79.2			C

4.02-d period originally proposed by Levato et al. (1991). To check this result, we added a set of 56 older, lower-resolution RV measurements to our high-resolution data, thereby extending the time span of our data set to 24 yr (8783 d). The analyses of this extended time series clearly confirm the conclusions from our high-resolution data set (see Fig. 2), slightly reducing the uncertainty on the period to (4.0157 ± 0.0002) d.

Table 2. Spectral lines used for the RV determination within the disentangling procedure.

Primary	Secondary
Violet domain	
He I λ 4026	He I λ 4026
Si IV λ 4089	
H I λ 4102	H I λ 4102
He II λ 4200	
Blue domain	
He I λ 4471	He I λ 4471
Mg II λ 4481	Mg II λ 4481
He II λ 4542	
	Si III λ 4553
	Si III λ 4568
	O II λ 4591
He II λ 4686	
He I λ 4713	He I λ 4713

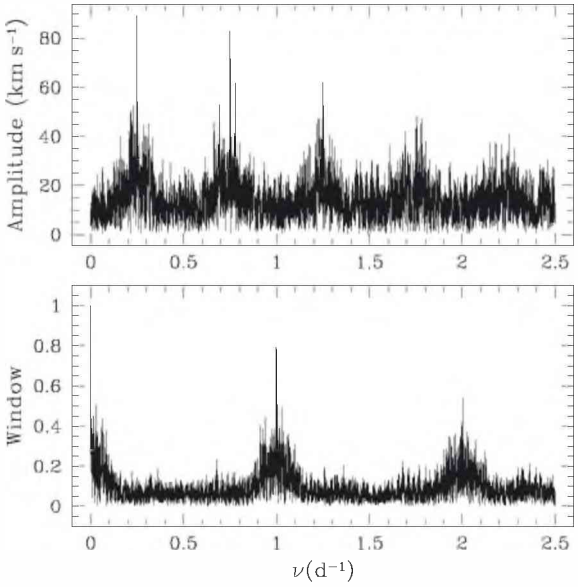

Figure 2. Top panel: periodogram (semi-amplitude spectrum) of the entire time series of 98 RVs of the primary component of Tr 16-112 computed with the method of Heck et al. (1985). Bottom panel: spectral window corresponding to our time series.

As a next step, we used the Liège Orbital Solution Package (LOSP) based on the method of Wolfe, Horak & Storer (1967) revised by Sana, Gosset & Rauw (2006), to compute the SB1 and SB2 orbital solutions of Tr 16-112. For the SB1 solution, we used the RVs of the primary's He II lines as measured on the entire set of high-resolution echelle spectra, whilst we adopted the RVs derived from the disentangling method applied to the FEROS spectra for the SB2 solution. The corresponding RV curves are shown in Fig. 3 and the parameters of the orbital solutions are listed in Table 3. Note that leaving the orbital period as a free parameter did not change the quality of the orbital solution.

The mass ratio (primary/secondary) is found to be 3.49 ± 0.08. To our knowledge, this is one of the largest mass ratios found in an OB binary system to date. Our orbital solution confirms the exis-

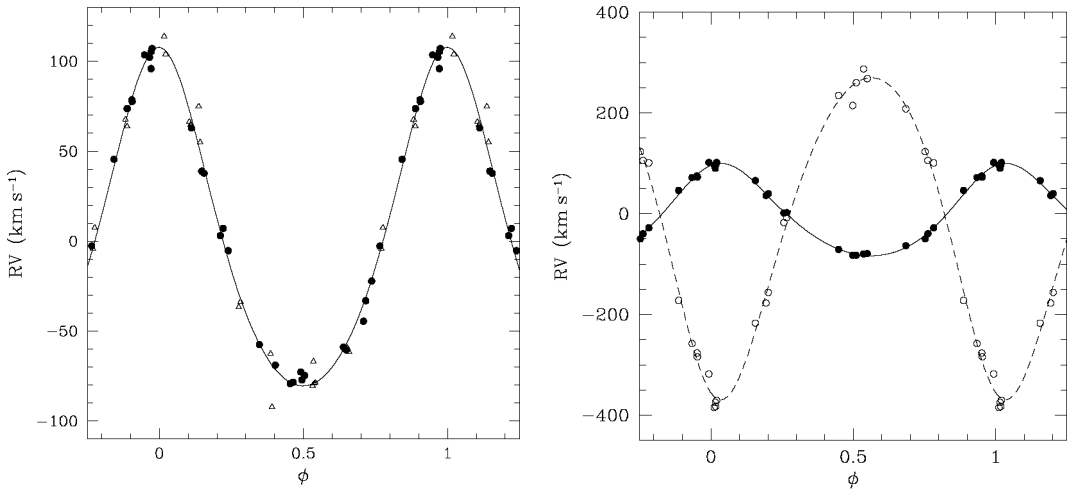

Figure 3. Left: SB1 RV curve of Tr 16-112 as derived from the RVs of the He II lines in the primary spectrum. The filled circles stand for the FEROS data, whilst the open triangles indicate RVs derived from the Casleo echelle spectra. Right: SB2 RV curve of Tr 16-112 as derived from the RVs obtained through the disentangling of the FEROS spectra. Filled symbols stand for the primary whilst the open symbols indicate the secondary star. The orbital solutions shown are described in Table 3. Phase $\phi = 0.0$ corresponds to the periastron passage.

Table 3. Orbital parameters of the SB1 (left) and SB2 (right) solutions of Tr 16-112. T_0 yields the time of periastron passage. The quoted uncertainties correspond to the 1σ error bars.

	SB1	SB2	
	Primary	Primary	Secondary
Period (d)	4.0157 (fixed)	4.0157 (fixed)	
γ (km s^{-1})	-1.3 ± 1.0	-4.9 ± 1.5	-2.9 ± 2.9
K (km s^{-1})	94.3 ± 1.5	91.7 ± 1.5	319.7 ± 5.1
e	0.16 ± 0.02	0.15 ± 0.01	
ω (°)	1.1 ± 5.6	342.8 ± 5.6	
$a \sin i$ (R$_\odot$)	7.38 ± 0.12	7.19 ± 0.12	25.05 ± 0.40
T_0 (HJD)	2454560.504 ± 0.059	2454560.310 ± 0.060	
$f(m)$ (M$_\odot$)	0.335 ± 0.016		
$m \sin^3 i$ (M$_\odot$)		21.7 ± 0.9	6.2 ± 0.2
$\overline{\lvert O-C \rvert}$ (km s^{-1})	4.7	3.8	12.4

tence of a significant eccentricity, although it is less extreme than previously thought. Note that most parameters agree reasonably well between the SB1 and SB2 orbital solutions, except for the longitude of periastron which has a rather large uncertainty. Comparing the relatively large minimum mass of the secondary with the typical masses of B2 stars suggests that the orbital inclination could be as large as 60°. Under these circumstances, grazing eclipses could a priori be possible.

4.3 Photometric data

Our photometric data reveal that Tr 16-112 displays low-level variations in its light curve with an amplitude of about 0.03 mag. When folded with the ephemeris found from the RV curve, we note that our observations actually miss the phase when secondary eclipse would be expected (around $\phi = 0.842$) but cover the phase where primary eclipse would occur ($\phi = 0.251$). The photometric data reveal no trace of an eclipse at this orbital phase and we thus conclude that Tr 16-112 does not display photometric eclipses. Rather the low-level photometric variability must be due to the ellipsoidal shapes of the stars.

We analysed the light curve of this system by means of the NIGHTFALL code[5] developed and maintained by R. Wichmann, M. Kuster and P. Risse. This software uses a Wilson-Devinney like iterative approach to solve the light curves of close binary systems in the Roche geometry, generalized to deal with the more complex situation of eccentric binaries where the sizes of the Roche lobes (and hence the values of the filling factors) change with orbital phase (see Kopal 1989). Despite the limited phase coverage and the small amplitude of the variations, we can attempt to get a decent fit of the data by varying the relevant model parameters which are in this case the orbital inclination, as well as the primary and secondary filling factors, defined as the ratio between the polar radius of the star and the polar radius of the Roche lobe at periastron passage.

We set the effective temperature of the primary star to 39000 K (Martins, Schaerer & Hillier 2005a) whilst the secondary temperature was fixed to 22 000 K according to the Schmidt-Kaler (1982) calibration, which seems reasonable for B2 main-sequence stars (Fitzpatrick & Massa 2005). The mass ratio, the orbital eccentricity as well as the longitude of periastron were fixed at the values derived

[5]http://www.hs.uni-hamburg.de/DE/Ins/per/Wichmann/Nightfall.html

Table 4. Parameters of the best-fitting model for the light curve of Tr 16-112. The error bars correspond to the 90 per cent confidence intervals. The average residual of the fit amounts to $\overline{O-C} = 0.005$ mag.

	Primary	Secondary
i (°)	54^{+4}_{-3}	
$T_{\rm eff}$ (K)	39 000 (fixed)	22 000 (fixed)
Periastron Roche lobe filling factor	$0.73^{+0.01}_{-0.02}$	$0.55^{+0.09}_{-0.11}$
m ($M_\odot$)	41.0 ± 2.5	11.7 ± 0.6
Mean radius R ($R_\odot$)	13.5 ± 0.6	5.7 ± 1.1
$\log L/L_\odot$	5.57 ± 0.04	3.83 ± 0.16

from the RV curve (see Table 3). The NIGHTFALL code was applied to the data in the V band since they are more numerous (996 data points) and of the highest quality. Due to the limited phase coverage of the data and the small range of variability, the parameters are actually not that well constrained. To evaluate the uncertainties on the model parameters, we systematically explored the parameter space, fixing one parameter at once, and searching for the combinations of the other two parameters that yield the lowest residuals.

The best-fitting value of the orbital inclination is found to be 54°. This then corresponds to absolute masses of $(41.0 \pm 2.5)\,M_\odot$ and $(11.7 \pm 0.6)\,M_\odot$ for the primary and secondary, respectively.

Given the rather large difference in temperature (and thus in surface brightness) between the primary and the secondary, the fit of the light curve is not very sensitive to the value of the secondary filling factor. As a result, the light curve does not allow us to effectively constrain the brightness ratio of the two stars independently of the results obtained from the spectroscopy. The situation is better for the primary (which dominates the light of the system). For this component, we can constrain the filling factor to be in the range 0.72–0.74 with a preferred value of 0.73.

We emphasize that the parameters in Table 4 should be taken as a first estimate only. A more extensive, higher quality (ideally space-borne), photometric campaign would be needed to fill in the gaps in the light curve and ascertain these numbers. Here, we only wish to stress that the observed light curve can be explained through ellipsoidal variations (Fig. 4). Pending confirmation of these parameters by future studies, we note that the primary is slightly more massive, significantly larger and brighter than a 'typical' main-sequence star of the same spectral type. In fact, these parameters would be more representative of luminosity class III objects (Martins et al. 2005a), although this would be at odds with the presence of the strong He II λ 4686 absorption in the primary spectrum. This would then suggest that Tr 16-112 is actually a slightly evolved object, contrary

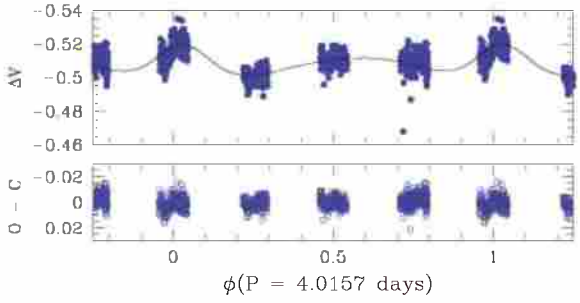

Figure 4. Light curve of Tr 16-112 in the V band (top panel). The solid curve yields the best-fitting model where the variations are due to the ellipsoidal shape of the primary star filling part of its critical volume in an eccentric binary. The parameters of the fit are listed in Table 4. The residuals are shown in the bottom panel.

to systems such as Tr 16-104 (Paper III) or FO 15 (Paper VI). Another point worth mentioning is that if the above parameters are indeed confirmed and if the reddening law towards this star is characterized by the typical value of the Trumpler 16 cluster ($R_V = 3.48 \pm 0.33$; see Carraro et al. 2004), then the distance modulus of Tr 16-112 would be 13.0 ± 0.3 (i.e. corresponding to a distance of 4.0 kpc), almost twice the distance inferred from the study of several eclipsing binaries in Tr 16 (e.g. Tr 16-1, Freyhammer et al. 2001 and Tr 16-104, Paper III). Whilst this is a surprising result, we have to recall that our line-of-sight towards the Carina region is actually roughly along the Sagittarius–Carina spiral arm, so that several distinct populations of massive stars could be seen projected on the same area of the sky. In the case of the eclipsing binary FO 15 (Paper VI), a similar contradiction was solved by showing that the latter star is subject to a highly anomalous extinction with $R_V = 4.15$. We note that for Tr 16-112, there is currently no evidence for such a large value of R_V. In addition, since the $E(B-V)$ colour excess of Tr 16-112 is much lower than for FO 15, adopting $R_V = 4.15$ for Tr 16-112 results in a reduction of the distance modulus of 20 per cent only.

5 HD 93343, A PECULIAR BINARY SYSTEM

Based on 10 low-dispersion spectra, Levato et al. (1991) reported RV variations of HD 93343 (O8 Vn) although they could not provide firm evidence for the multiplicity of the star. Later on, an abstract reporting a very preliminary SB1 orbital solution ($P_{\rm orb} \sim 44$ d, $e \sim 0.39$, $K_1 \simeq 71$ km s^{-1}) was presented by Solivella & Niemela (1998).

Here, we analyse six medium-resolution B&C and nine high-resolution FEROS spectra of HD 93343 spread over 6 yr. These data reveal the SB2 nature of this star: one of the components of HD 93343 has narrow absorption lines [full width at half-maximum (FWHM) $\sim$125 km s^{-1}], whilst the companion displays much broader lines (FWHM $\sim$500 km s^{-1}!). As can be seen in Fig. 5, the sharper lines obviously move in RV. The RV changes of the broad lines are less obvious to see. However, simultaneous fits of two Gaussians to the observed profiles clearly indicate that the

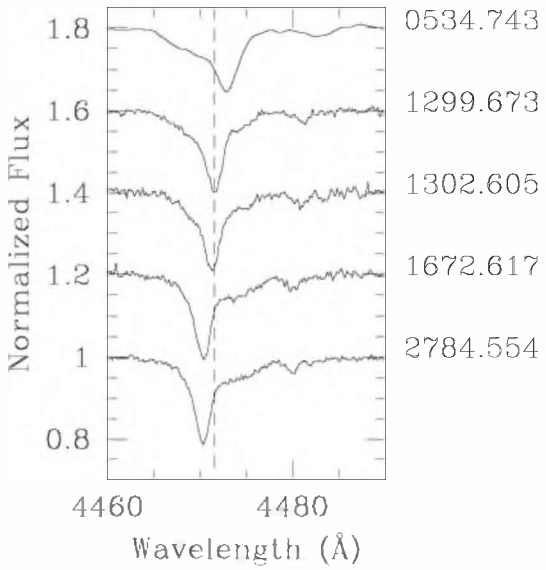

Figure 5. Montage of several of the He I λ 4471 profiles observed in the spectrum of HD 93343. The date of the observation is indicated on the right in the format HJD−245 0000.

broad lines move in phase opposition with the narrow lines, although their RVs are affected by large uncertainties (at least 20 km s^{-1}) due to their widths. Our RV data allow us to establish a preliminary estimate of the mass ratio of the system $m_{\rm narrow}/m_{\rm broad} = 0.63 \pm 0.06$.

The apparent EWs (i.e. with respect to the combined primary + secondary continuum) of the He I λ 4471 line as determined from the two Gaussian fits are 0.57 ± 0.02 and 0.23 ± 0.05 Å for the broad and narrow-line component, respectively. For the He II λ 4542 lines, the apparent EWs are 0.41 ± 0.05 and 0.17 ± 0.04 Å, respectively. From these numbers, we infer a spectral type O8 for both stars (log $W' = 0.14 \pm 0.06$ for the broad-line component and log $W' = 0.11 \pm 0.14$ for the star with the sharper lines; see Conti 1973b and Mathys 1988). We note that the spectral type of the component with the sharper lines could actually be in the range O7–8.5. The same EWs allow us to estimate that the broad-line component should be roughly 2.4 times brighter in the optical than the narrow-line component. Unfortunately, an attempt to disentangle the spectra of the two stars failed because the RV changes sampled by our data do not cover the full width of the broad lines. In such a situation, the disentangling method cannot recover the spectra of the components (see González & Levato 2006).

The likely combination of a slow and fast rotator in HD 93343 is reminiscent of the situation encountered in Plaskett's Star (HD 47129; see Linder et al. 2008) and this system could thus provide an interesting test case for binary evolution theories (e.g. de Mink et al. 2009). Unfortunately, the existing data are not sufficient to establish a full orbital solution. From the RV changes observed over six consecutive nights in 1997 March and 1999 May (see Table 5), we can guess that the orbital period is likely of the order of a few weeks. A very preliminary Fourier analysis indicates the presence of several alias peaks of identical amplitude in the periodogram for periods around 40–50 d, with the highest one corresponding to a period of 44.54 d. We note that the latter result is in good agreement with the preliminary period reported by Solivella & Niemela (1998).

We finally analysed an extensive set of 6101 V-band photometric measurements of HD 93343 taken between 2004 June and 2008 April with the same instrumentation as for Tr 16-112. Although the photometric variations are rather small, the Heck et al. (1985) periodogram actually presents its highest peak for a period of 44.15 d with a peak-to-peak amplitude of 0.016 mag. Whilst another peak with almost identical amplitude is found in the periodogram for a period of 80.3 d, we nevertheless conclude that the orbital period of HD 93343 is indeed likely to be around 44 d. We stress that the light curve folded with a period of 44.15 d indicates a single modulation per cycle (see Fig. 6) unlike what one would expect for purely ellipsoidal variations assuming the system has a circular orbit. A modelling of these photometric variations must however await the results of a more extensive spectroscopic (and photometric) monitoring campaign of this system.

Table 5. RVs of HD 93343 as inferred from a simultaneous fit of two Gaussians to the He I λλ 4471, 4921, 5876 and He II λ 4542 line profiles observed in our data. Note that for the B&C spectra, only the He I λ 4471 and He II λ 4542 lines were measured.

HJD−245 0000	Narrow lines	Broad lines	Inst.
534.743	−52.5	101.0	B&C
535.749	−55.8	87.7	B&C
536.716	−47.9	63.0	B&C
537.731	−32.2	53.9	B&C
538.715	−50.9	47.4	B&C
539.717	−38.3	42.4	B&C
1299.673	4.8	−20.6	F
1300.677	0.2	−27.4	F
1301.630	−9.5	−19.4	F
1302.605	−22.7	−6.7	F
1304.650	−30.0	13.0	F
1670.632	−79.2	70.5	F
1672.617	−81.3	60.7	F
2783.550	−80.5	49.1	F
2784.554	−81.3	59.3	F

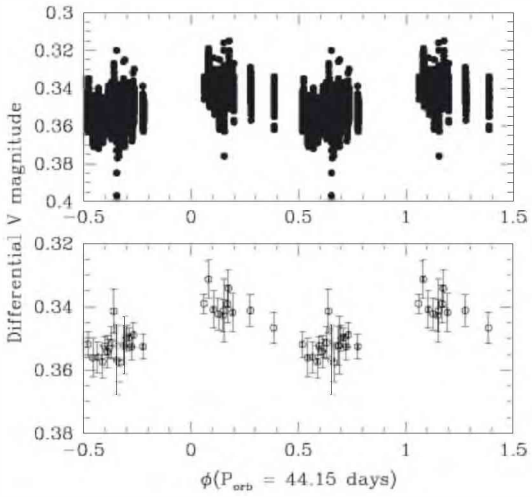

Figure 6. Photometric variations of HD 93343. The top panel illustrates the raw data (ΔV) folded with a period of 44.15 d. Phase zero was arbitrarily set to HJD 245 0000. The bottom panel yields the same light curve, but where the data of each single observing night have now been averaged. The error bars on the data yield the dispersion of ΔV about the mean for each observing night.

6 THE RV CONSTANT STAR HD 93250

Last but not least, HD 93250 (O3.5; Walborn et al. 2002) was considered to have a constant RV by Levato et al. (1991). This statement was based on nine low-resolution spectra obtained on nine consecutive nights. The 1σ dispersion of their RV measurements was 11.6 km s^{-1}. However, some indirect indications of a possible binarity were found in the radio and X-ray domains. In fact, Leitherer, Chapman & Koribalski (1995) reported on an Australia Telescope Compact Array radio observation of HD 93250. The star was detected only at the 8.64-GHz frequency. Assuming the radio flux to be of thermal origin and adopting a distance of 2.2 kpc, Leitherer et al. (1995) inferred a mass-loss rate of log $\dot{M} \sim -4.39 \pm 0.15$, considerably larger than the value derived from analyses of the optical spectra of this star[6]. Therefore, Leitherer et al. (1995) suggested that the radio emission is essentially non-thermal. Since non-thermal (synchrotron) radio emission is nowadays commonly associated with a wind–wind collision in an early-type binary (see e.g. De Becker 2007), one would thus expect HD 93250 to be a binary system. Some hints for binarity come also from the X-ray domain. Indeed, *Chandra* observations revealed that this star has the

[6]Indeed, Martins et al. (2005b) subsequently derived log $\dot{M} = -6.25 \pm 0.7$ from a model atmosphere fit.

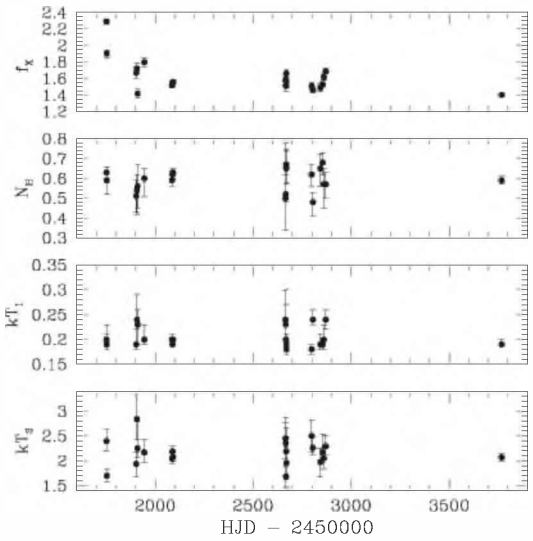

Figure 7. From top to bottom, the various panels show the observed X-ray flux of HD 93250 (in units 10^{-12} erg cm^{-2} s^{-1}) over the 0.5–10 keV domain, the wind hydrogen column density (in units 10^{22} cm^{-2}) in addition to the interstellar column of 2.55×10^{21} cm^{-2}, the temperatures of the first and second thermal component (in keV).

largest $\log L_X/L_{bol}(= -6.5)$ among the objects studied in this paper (Sanchawala et al. 2007). Moreover, the star has been frequently observed with *XMM–Newton* in the course of various campaigns on the Carina region. In the framework of a global study of the X-ray properties of OB stars (Nazé 2009), we have retrieved and analysed 21 *XMM–Newton*-EPIC spectra of HD 93250 from the 2XMM catalogue (Watson et al. 2009). The X-ray flux of HD 93250 displays clear variability between the different pointings (see Fig. 7), whilst most single O-type stars usually exhibit a rather constant X-ray flux. The EPIC spectra of HD 93250 can be fitted with a two-temperature optically thin thermal plasma mekal model with temperatures around 0.20 keV and 1.7–2.8 keV. These results, i.e. the existence of a relatively hard thermal component and the significant X-ray variability could be seen either as further evidence for HD 93250 being a colliding wind binary or alternatively they could indicate that this star harbours a magnetically confined wind similar to θ^1 Ori C (Gagné et al. 2005).

Six FEROS high-resolution spectra of HD 93250 were analysed. The spectrum of this star displays several emission lines: N III λλ 4634-40, C III λλ 5696, 6721, 6727-31 and Si IV λλ 4089, 4116 are the most prominent ones. A weak N IV λ 4058 emission is also seen, whilst He II λ 4686 is in strong absorption (EW = 0.54 ± 0.06 Å) with a slightly asymmetric profile. These features indicate that HD 93250 is an O V((f$^+$)) star. Walborn et al. (2002) introduced the new O3.5 spectral type and proposed HD 93250 to be a prototype of this category. This result is in good agreement with the ratio of the EWs of the He I λ 4471 (EW = 0.119 ± 0.008 Å) and He II λ 4542 (EW = 0.690 ± 0.018 Å) classification lines. The Conti (1973b) criterion yields $\log W' = -0.76 \pm 0.03$ corresponding to an O4 spectral type[7]. In summary, HD 93250 hence appears to be an O3.5 V((f$^+$)) star.

Our RV measurements indicate 1σ RV dispersions of less than 2.0 km s^{-1} for the He I λ 4471, He II λλ 4542 and 5412 absorption lines. The same conclusion holds if we consider the mean RV of seven lines ($\sigma = 1.3$ km s^{-1}, see Table 6). Note that the largest variability ($\sigma = 6.5$ km s^{-1}) is found for the He II λ 4686 line. This is no surprise since this line shows some hints for a P-Cygni type profile and the variability is thus most likely due to variations of the stellar wind. For comparison, the RV dispersion of the DIB at 5780 Å amounts to 0.7 km s^{-1}. Therefore, we conclude that no significant RV variations are observed for the photospheric lines of HD 93250. Our measurements sample time-scales of 3–5 d as well as of several years. The lack of significant RV variations therefore indicates that HD 93250 is most likely not a spectroscopic binary with an orbital period of the order of a few days to a few weeks or a few years. Finally, it should be noted that Mason et al. (1998) did not report a visual companion to HD 93250. In conclusion, HD 93250 is probably either a single star or a moderately wide binary system seen under a low-inclination angle.

[7]Note that Conti (1973b) did not consider an O3.5 spectral type in his classification scheme.

Table 6. RVs of HD 93250 as measured from the He I λλ 4471, 5876, He II λλ 4026, 4200, 4542, 5412 and O III λ 5592 absorption lines.

HJD−245 0000	Mean RV
1304.551	−9.9
2782.538	−9.1
2784.526	−12.5
3130.501	−9.2
3131.455	−9.3
3133.454	−10.5

7 O-TYPE BINARIES IN AND AROUND THE TRUMPLER 16 CLUSTER

In this section, we briefly discuss some of the results obtained so far in the course of the optical campaign of the X-Mega project. In addition to the stars studied in this paper, we include the results on some other stars: Tr 16-34, HD 93205, Tr 16-104, Tr 16-110, HD 93161, FO 15 taken from the previous papers of this series (Paper I; Paper IV; Paper II; Paper III; Paper V; Paper VI) as well as Tr 16-1 and HD 93403 from the work by Freyhammer et al. (2001) and Rauw et al. (2000), respectively (see Table 7).

The properties of the eclipsing systems, Tr 16-1, Tr 16-104 and FO 15 (Freyhammer et al. 2001; Paper III; Paper VI), are particularly useful since their light curve and orbital solution provide absolute parameters and allow us to constrain their distance. Indeed, the investigations of these three eclipsing systems agree with a distance of about 2.5 kpc. For the ellipsoidal variables, Tr 16-112 and HD 93205, the uncertainties on the orbital inclination and hence on the absolute parameters are much larger (Antokhina et al. 2000 and this work).

For the non-eclipsing binaries and for the probably single star HD 93250, we have assumed a distance of 2.5 kpc. For each star, we have evaluated the effective temperature and the bolometric corrections according to Martins et al. (2005a) and Martins & Plez (2006). We have generally assumed an uncertainty of half a spectral type. To derive the luminosities, we need the observed magnitude, the reddening, the brightness ratios between the different components, the bolometric corrections and an estimate of the distance. The observed magnitudes and colours were taken from the WEBDA data base (http://www.univie.ac.at/webda/). The relative brightness of the components of the binary systems was estimated in the various papers from the ratio of the EWs of the primary and

Table 7. Orbital properties of the short-period spectroscopic binaries in the Carina complex. For the third component of the triple system Tr 16-104, the two possible solutions are listed (see Paper III). In the last column, SB1 and SB2 stand, respectively, for a single-lined and a double-lined spectroscopic binary, whilst the e and v letters indicate systems that are known to display photometric eclipses or ellipsoidal variations, respectively.

System	Spectral types	P_{orb} (d)	e	ω (°)	$q = m_2/m_1$	Type
Tr 16-1	O9.5 V + B0.3 V	1.4693	0.0	–	0.83 ± 0.08	SB2e
Tr 16-34	O8 V + O9.5 V	2.3000	0.0	–	0.76 ± 0.01	SB2
HD 93205	O3 V + O8 V	6.0803	0.371 ± 0.005	50.6 ± 0.9	0.42 ± 0.01	SB2v
Tr 16 – 104	O7 V + O9.5 V + B0.2IV	2.1529	0.0	–	0.65± 0.03	SB2e
		285, 1340	0.25 ± 0.05, 0.37 ± 0.04	287 ± 20, 238 ± 8		SB1
Tr 16 – 110	O7 V + O8 V	3.6284	0.06 ± 0.03	355 ± 15	0.96 ± 0.04	SB2
	O9 V	5.034	0.09 ± 0.04	209 ± 30		SB1
HD 93161A	O8 V + O9 V	8.566	0.0	–	0.76 ± 0.01	SB2
FO 15	O5.5 V + O9.5 V	1.1414	0.0	–	0.52 ± 0.04	SB2e
Tr 16-112	O5.5 V + B2 V-III	4.0157	0.15 ± 0.01	342.8 ± 5.6	0.29 ± 0.01	SB2v
HD 93403	O5.5 I + O7 V	15.093	0.23 ± 0.02	22.5 ± 4.4	0.57 ± 0.02	SB2

Table 8. Revised temperatures and bolometric luminosities of the components of eclipsing binaries (top part), the ellipsoidal variables (second part), the non-eclipsing binaries (third part) and two presumably single O-stars (lower part) in the Carina complex.

System	Spectral type	T_{eff} (K)	$\log L/L_\odot$
Tr 16-1a	O9.5 V	32000 ± 500	4.42 ± 0.06
Tr 16-1b	B0.3 V	30000 ± 800	4.14 ± 0.07
Tr 16-104a	O7 V	36900 ± 1000	4.92 ± 0.11
Tr 16-104c	O9.5 V	31900 ± 1000	4.34 ± 0.09
FO 15a	O5.5 V	40000 ± 1000	5.09 ± 0.01
FO 15b	O9.5 V	32000 ± 500	4.41 ± 0.01
HD 93205a	O3.5 V	43900 ± 1000	5.32 ± 0.14
HD 93205b	O8 V	34900 ± 1000	4.71 ± 0.10
Tr 16-112a	O5.5-6 V	39000 ± 1000	5.57 ± 0.04
Tr 16-112b	B2 V-III	22000 ± 1500	3.83 ± 0.16
HD 93161Aa	O8 V	34900 ± 1000	5.16 ± 0.04
HD 93161Ab	O9 V	32900 ± 1000	4.85 ± 0.06
HD 93343a	O8 V	34900 ± 1000	4.86 ± 0.12
HD 93343b	O7-8.5 V	34900 ± 1000	4.48 ± 0.12
HD 93403a	O5.5 I	37700 ± 900	5.72 ± 0.05
HD 93403b	O7 V	36900 ± 1000	4.97 ± 0.22
Tr 16-34a	O7.5 V	35900 ± 1000	4.89 ± 0.09
Tr 16-34b	O9 V	32900 ± 1000	4.44 ± 0.12
Tr 16-110a	O7 V	36900 ± 1000	4.86 ± 0.06
Tr 16-110b	O8 V	34900 ± 1000	4.69 ± 0.06
Tr 16-110c	O9 V	32900 ± 1000	4.55 ± 0.07
HD 93161B	O6.5 V(f)	37900 ± 1000	5.50 ± 0.04
HD 93250	O3.5 V((f$^+$))	44000 ± 300	6.09 ± 0.07

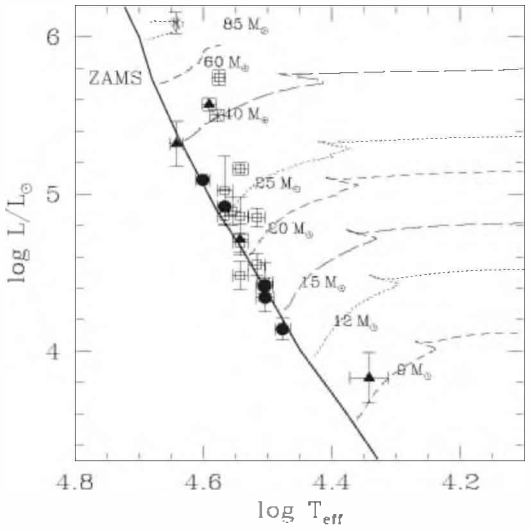

Figure 8. Location in the Hertzsprung–Russell diagram of the components of various early-type systems of the Carina region. Eclipsing binaries are shown by filled dots, whilst ellipsoidal variables are shown as filled triangles. Non-eclipsing binary systems are indicated by open squares and the asterisks stand for two probably single stars. The single star evolutionary tracks from Meynet & Maeder (2003) for an initial rotational velocity of 300 km s^{-1} at solar metallicity are shown for those parts of the tracks where the surface hydrogen abundance $X \geq 0.4$.

secondary lines. The reddening was evaluated according to the results of Carraro et al. (2004). These authors argued that a unique reddening law is not appropriate to study the whole Carina region and they estimated different values of the selective extinction $R_V = A_V/E(B-V)$ for each cluster.

This approach yields the bolometric luminosities quoted in Table 8. For Tr 16-112, we use the luminosities derived from the light curve analysis, rather than assuming a distance of 2.5 kpc. The luminosity of HD 93161B might be overestimated if the star turned out to be indeed another binary system (see Paper V). Note that for HD 93403, the evolutionary masses are revised downwards compared to the previous analysis (Rauw et al. 2000) and the evolutionary mass ratio is now in better agreement with the observed value (1.75 ± 0.06). Finally, we stress that the bolometric luminosity of HD 93250 that we obtain through our approach ($\log L/L_\odot = 6.09 \pm 0.07$) is in very good agreement with the luminosity $\log L/L_\odot = 6.12^{+.25}_{-.17}$ inferred by Martins et al. (2005b) using a different method.

In Fig. 8, we have plotted the various stars of Table 8 in a Hertzsprung–Russell diagram along with the evolutionary tracks from Meynet & Maeder (2003) for solar metallicity. Provided that all stars (except maybe Tr 16-112) are indeed at the same distance from Earth, this diagram suggests that the components of HD 93161 and HD 93403 are evolved off the zero-age main-sequence (ZAMS) with an age of about 2–3 Myr, unlike the components of the eclipsing binaries and of Tr 16-110 which are found very close to the ZAMS.

Using all the available orbital solutions for early-type binary systems in or around Trumpler 16, we constructed the period–eccentricity diagram shown in Fig. 9. This figure confirms our assertion from Fig. 8 that HD 93161A must be older and more

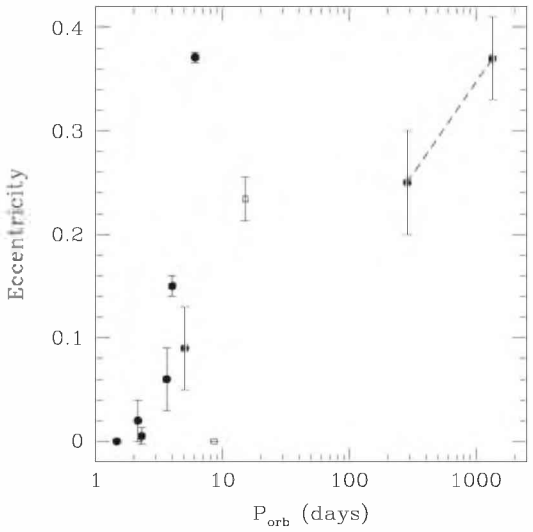

Figure 9. Eccentricity of the orbits of a sample of early-type binaries in the Carina complex as a function of the orbital period. The probable members of Tr 16 are shown by filled symbols, whereas the two binary systems outside the cluster (HD 93403 and HD 93161A) are indicated by open symbols. For the third component of the triple system Tr 16-104, the two possible solutions are shown, connected by a dotted line.

evolved than the main-sequence stars in the core of Tr 16. In fact, for the latter, significant eccentricities are found for orbital periods as short as ∼4 d, indicating that tidal interactions have not yet had the time to circularize the eccentric orbits.

At least three triple or higher multiplicity systems were found among the early-type stars in the Carina complex. Concerning the fraction of systems of higher multiplicity, Tokovinin (2004) found that about 43 per cent of the nearby low-mass (0.5–1.5 $M_{\odot}$) spectroscopic binaries with $P < 10$ d quoted in the Eighth Catalogue of Spectroscopic Binaries have indeed a tertiary component. The third component provides a natural sink for the angular momentum that needs to be removed from a binary system in order to make it a close one. Tokovinin (2004) quotes an empirical stability limit for a triple system:

$$P_{\rm out}(1-e_{\rm out})^{3} > 5\,P_{\rm in},$$

where $P_{\rm in}$, $P_{\rm out}$ and $e_{\rm out}$ correspond, respectively, to the orbital period of the close binary, the orbital period of the third star around the centre of mass of the close binary and the eccentricity of the third star's orbit. Both possible orbital solutions for the third component in Tr 16-104 largely satisfy this criterion, whilst the orbital period of the SB1 component in Tr 16-110 assumed to correspond to $P_{\rm out}$ of a triple system obviously cannot meet this condition, thus confirming the idea that there should exist a fourth (unseen) component in this system.

8 CONCLUSIONS

In this paper, we have presented the very first SB2 orbital solution of the Tr 16-112 binary system. We derived a rather large mass ratio and confirmed that this binary has an orbit with a significant eccentricity despite of its short orbital period. This system displays ellipsoidal variations that can be explained by the primary filling about 73 per cent of its Roche lobe at periastron. Furthermore, we have presented the first clear evidence for an SB2 signature in the spectrum of HD 93343. This system likely harbours one fast and one slow rotator and could currently be in a post-Roche lobe overflow evolutionary stage, making it a somewhat less extreme version of Plaskett's Star. Finally, we have shown that the properties of the components of most of the binaries in the Carina region (in or around Trumpler 16) suggest that these are very young objects where tidal interactions have not yet had the time to circularize the orbits. One point that remains to be studied in the forthcoming years is the lack of a clear binary signature in HD 93250. This system displays a non-thermal radio emission and such a phenomenon is a priori not expected for a single star. Interferometric observations could help to search for a companion that might be either too faint or too far away from the O3.5 primary to be detected in spectroscopy.

ACKNOWLEDGMENTS

We thank the referee of this paper for his constructive comments. The Liège team acknowledges multiple support from the Fonds de Recherche Scientifique (FRS/FNRS), through the XMM/INTEGRAL PRODEX contract as well as by the Communauté Française de Belgique – Action de recherche concertée – Académie Wallonie - Europe.

REFERENCES

Albacete Colombo J. F., Morrell N. I., Niemela V. S., Corcoran M. F., 2001, MNRAS, 326, 78 (Paper I)
Albacete Colombo J. F., Morrell N. I., Rauw G., Corcoran M. F., Niemela V. S., Sana H., 2002, MNRAS, 336, 1099 (Paper IV)
Antokhina E. A., Moffat A. F. J., Antokhin I. I., Bertrand J.-F., Lamontagne R., 2000, ApJ, 529, 463
Carraro G., Romaniello M., Ventura P., Patat F., 2004, A&A, 418, 525
Conti P. S., 1973a, ApJ, 179, 161
Conti P. S., 1973b, ApJ, 179, 181
Corcoran M. F., Pittard J. M., Marchenko S. V., The X-Mega Group, 1999, in van der Hucht K. A., Koenigsberger G., Eenens P. R. J., eds, Proc. IAU Symp. 193, Wolf–Rayet Phenomena in Massive Stars and Starburst Galaxies. Astron. Soc. Pac., San Francisco, p. 772
De Becker M., 2007, A&AR, 14, 171
de Mink S. E., Cantiello M., Langer N., Pols O. R., Brott I., Yoon S.-Ch., 2009, A&A, 497, 243
Didelon P., 1982, A&AS, 50, 199
Feinstein A., Marraco H. G., Muzzio J. C., 1973, A&AS, 12, 331
Fitzpatrick E. L., Massa D., 2005, AJ, 129, 1642
Freyhammer L. M., Clausen J. V., Arentoft T., Sterken C., 2001, A&A, 369, 561
Gagné M., Oksala M. E., Cohen D. H., Tonnesen S. K., ud-Doula A., Owocki S. P., Townsend R. H. D., MacFarlane J. J., 2005, ApJ, 628, 986
González J. F., Levato H., 2006, A&A, 448, 283
Gosset E., Royer P., Rauw G., Manfroid J., Vreux J.-M., 2001, MNRAS, 327, 435
Heck A., Manfroid J., Mersch G., 1985, A&AS, 59, 63
Howarth I. D., Siebert K. W., Hussain G. A. J., Prinja R. K., 1997, MNRAS, 284, 265
Kopal Z., 1989, The Roche Problem. Kluwer, Dordrecht
Lafler J., Kinman T. D., 1965, ApJS, 11, 216
Leitherer C., Chapman J. M., Koribalski B., 1995, ApJ, 450, 289
Levato H., Malaroda S., Morrell N., Garcia B., Hernández C., 1991, ApJS, 75, 869
Linder N., Rauw G., Martins F., Sana H., De Becker M., Gosset E., 2008, A&A, 489, 713
Luna G. J., Levato H., Malaroda S., Grosso M., 2003, Inf. Bull. Var. Stars, 5375, 1
Martins F., Plez B., 2006, A&A, 457, 637
Martins F., Schaerer D., Hillier D. J., 2005a, A&A, 436, 1049
Martins F., Schaerer D., Hillier D. J., Meynadier F., Heydari-Malayeri M., Walborn N. R., 2005b, A&A, 441, 735

Mason B. D., Gies D. R., Hartkopf W. I., Bagnuolo W. G. Jr, ten Brummelaar T., McAlister H. A., 1998, AJ 115, 821
Mathys G., 1988, A&AS, 76, 427
Meynet G., Maeder A., 2003, A&A, 404, 975
Morrell N. I. et al., 2001, MNRAS, 326, 85 (Paper II)
Nazé Y., 2009, A&A, in press
Nazé Y., Antokhin I. I., Sana H., Gosset E., Rauw G., 2005, MNRAS, 359, 688 (Paper V)
Nazé Y., Walborn N. R., Martins F., 2008, Rev. Mex. Astron. Astrof., 44, 331
Niemela V. S., Morrell N. I., Fernández Lajús E., Barbá R., Albacete Colombo J. F., Orellana M., 2006, MNRAS, 367, 1450 (Paper VI)
Penny L. R., 1996, ApJ, 463, 737
Rauw G., Sana H., Gosset E., Vreux J.-M., Jehin E., Parmentier G., 2000, A&A, 360, 1003
Rauw G., Sana H., Antokhin I. I., Morrell N. I., Niemela V. S., Albacete Colombo J. F., Gosset E., Vreux J.-M., 2001, MNRAS, 326, 1149 (Paper III)
Sana H., Hensberge H., Rauw G., Gosset E., 2003, A&A, 405, 1063
Sana H., Gosset E., Rauw G., 2006, MNRAS, 371, 67
Sana H., Gosset E., Nazé Y., Rauw G., Linder N., 2008, MNRAS, 386, 447
Sanchawala K., Chen W.-P., Lee H.-T., Chu Y.-H., Nakajima Y., Tamura M., Baba D., Sato S., 2007, ApJ, 655, 462
Schmidt-Kaler T., 1982, Physical Parameters of the Stars. Landolt-Börnstein Numerical Data and Functional Relationships in Science and Technology, New Series, Group VI. Springer-Verlag, Berlin
Simón-Díaz S., Herrero A., 2007, A&A, 468, 1063
Solivella G. R., Niemela V. S., 1998, in Focal Points in Latin American Astronomy, IX Latin American Regional IAU Meeting
Tokovinin A., 2004, Rev. Mex. Astron. Astrof. Conf. Series, 21, 7
Walborn N. R., 1972, AJ, 77, 312
Walborn N. R., 1973, AJ, 78, 1067
Walborn N. R., 1982, ApJS, 48, 145
Walborn N. R., Fitzpatrick E. L., 1990, PASP, 102, 379
Walborn N. R. et al., 2002, AJ, 123, 2754
Watson M. G. et al., 2009, A&A, 493, 339
Wolfe R. H. Jr, Horak H. G., Storer N. W., 1967, in Hack M., ed., Modern Astrophysics. A Memorial to Otto Struve. Gordon & Breach, New York, p. 251

This paper has been typeset from a TEX/LATEX file prepared by the author.